

Contents list available at JMCS

Journal of Mathematics and Computer Science

Journal Homepage: www.tjmcs.com



A Fast Maximum Power Point Tracking for mismatching compensation for PV Systems under Normal and Partially Shaded Conditions

Mohammad Sarvi¹, Mandana Hojati Tabatabaee², Iman Soltani³

Electrical Engineering Department, Imam Khomeini International University, Qazvin, Iran

¹sarvi@ikiu.ac.ir, ²m_h_tabatabaee2007@yahoo.com, ³i_soltani@ikiu.ac.ir,

Article history:

Received May 2013

Accepted June 2013

Available online June 2013

Abstract

To increase the efficiency of photovoltaic (PV) systems, maximum power point tracking of the solar arrays is needed. Output power of solar arrays depends on the solar irradiance, temperature and load. Irradiance changing effects on current is more than voltage and with irradiance increasing, current increases more than voltage and finally power increases. But effect of temperature changing is more on voltage and with temperature increasing, voltage decreases and in result the power decreases. If solar array be under shade conditions, it's P-I characteristic has multiple peaks and finding of real maximum power point is a problem. This paper presents a fast maximum power point tracking with improved Particle Swarm Optimization for PV systems under normal and partially shaded conditions. Simulation results confirm that proposed MPPT algorithm and kinds of it with high accuracy can track the peak power point under different irradiation, temperature and partially shaded conditions and they have results near to real value.

Keywords- Maximum power point tracking, Photovoltaic system, Partial shading, Particle swarm optimization, DC/DC converter.

1. Introduction

As a kind of green energy with no pollution, no noise, inexhaustibility, solar energy gets more and more people's attention. Solar arrays are the primary source of photovoltaic systems. They are dependent power sources with nonlinear V-I characteristics under different environmental (irradiation, temperature and degradation) condition. Thus, Solar arrays output power will change with the load changes even in

determining external conditions, but there exists a maximum power point, as well as a voltage and current corresponding with the maximum power point .Two factors, array temperature (T) and irradiation (S), will affect the generated PV power significantly.[1]

When the work environment changes, especially the light intensity or ambient temperature changes, the solar cells output characteristic curve will change with it, and the maximum power point also changes correspondingly [2-3]. Solar arrays have high fabrication cost and low energy conversion efficiency. To increase the efficiency of photovoltaic systems, maximum power point tracker is an important component of these systems [4]. Different maximum power point tracking (MPPT) techniques have been reported[5] these methods vary in robustness, quality of dynamic response, validity, cost and complexity of implementation. So far there are roughly P&O methods[6], Incremental Conductance (IC) method[7,13], ripple correlation [8], short circuit current [9] Hill and Climbing method (H&C)[10], Voltage based Maximum Power Point Tracking (VMMPT) and Current based Maximum Power Point Tracking (CMPPT) methods[12], open-circuit voltage approaches [14] and intelligent computing method[15-21].

The Particle Swarm Optimization (PSO) algorithm is population- based optimization algorithm inspired by the social behavior of bird flocking and fish schooling where each individual is referred to as particle and represents a candidate solution [22]. PSO has higher accuracy and better response time than other ways. This paper presents IPSO based on maximum power point tracking of photovoltaic system under normal and partial shading conditions in addition temperature and irradiance changing conditions. PSO based MPP tracker uses conventional parameters and number of shaded cells in inputs and determines solar array current and voltage correspond to maximum power.

2. PV Module Characteristics Under Partial Shading Conditions

Solar cells operating point depends on the connected load to them. The current and voltage and therefore Power of one solar cell is limited, and thus solar cells are connected with each other in series and parallel for achieving the suitable and appropriate voltage and current. Using the equivalent circuit of Fig.1, the nonlinear V-I equation characteristic of a solar array with M parallel strings and N series cells per string is:

$$v_{SA} = \frac{N}{\lambda} \ln \left(\frac{MI_{ph} - i_{SA} + MI_0}{MI_0} \right) - \frac{N}{M} R_S i_{SA} \tag{1}$$

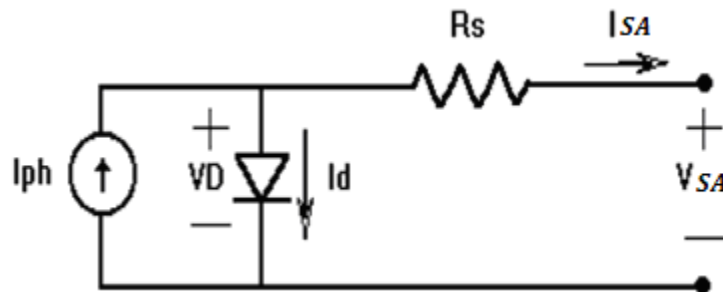


Fig.1. Equivalent circuit of solar cells.

Where v_{SA} and I_{SA} are the output voltage and current of the solar cell, respectively, I_{ph} is the generated current under a given irradiation condition, I_o is the reserve saturation current. Also $\lambda = q/AKT$ is a constant coefficient that q is the charge of an electron, A is the ideality factor for a p-n junction, K is the Boltzmann's constant, T is the temperature and R_s is the series resistance of the solar cell.

The V-I characteristics of solar arrays depend on the operating temperature and irradiation as demonstrated by the following equations:

$$(2) \Delta T = T - T_r$$

$$(3) \Delta i = \alpha(I_{sc} / I_{scr})\Delta T + (I_{sc} / I_{scr} - 1)I_{scr}$$

$$(4) \Delta v = -\beta\Delta T - R_s\Delta i$$

$$(5) v_{SA}^{new} = v_{SA} + \Delta v$$

$$(6) i_{SA}^{new} = i_{SA} + \Delta i$$

(7) $p_{SA} = v_{SA}^{new} \cdot i_{SA}^{new}$ Where T and T_r are the operating and the rated (nominal) solar panel temperatures, respectively, α is the current-temperature coefficient, β is the voltage-temperature coefficient and I_{sc} and I_{scr} are the operating and the rated solar panel short circuit currents, respectively, that is proportional to irradiation. For the silicon solar panel (with M=1, N=36) used for theoretical analysis of this paper. (Table 1, manufactured by the OFFC), Eq.(1) can be written as:

$$v_{SA} = k \ln\left(\frac{I_{ph} - i_{SA} + I_o}{I_o}\right) - i_{SA} \quad (8)$$

Table 1

Characteristics of the OFFC silicon solar array at T=25 °C.

Current-Temperature Coefficient	$\alpha = 0.002086 [A / ^\circ C]$
---------------------------------	------------------------------------

Voltage-Temperature Coefficient	$\beta = 0.0779 [V / ^\circ C]$
Reverse Saturation Current	$I_o = 0.5 \times 10^{-4} [A]$
Rated Short Circuit Current	$I_{sc} = 2.926 [A]$
Cell Resistance	$R_S = 0.0277 [\Omega]$
Cell Material Coefficient	$\lambda = 20.41 [V^{-1}]$

The generated current under a given irradiation level is given by the following equation:

$$I_{ph} = [I_{scr} + \alpha(T - T_r)](S / 1000) \tag{9}$$

Fig.2 shows the power-current (P-I) characteristic of the solar array according to the Irradiation (Fig.2 (a)) and temperature (Fig.2 (b)).

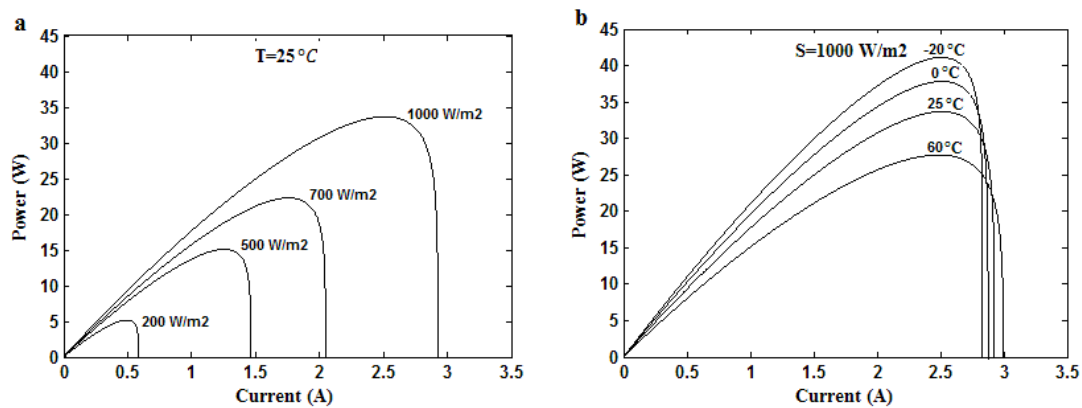
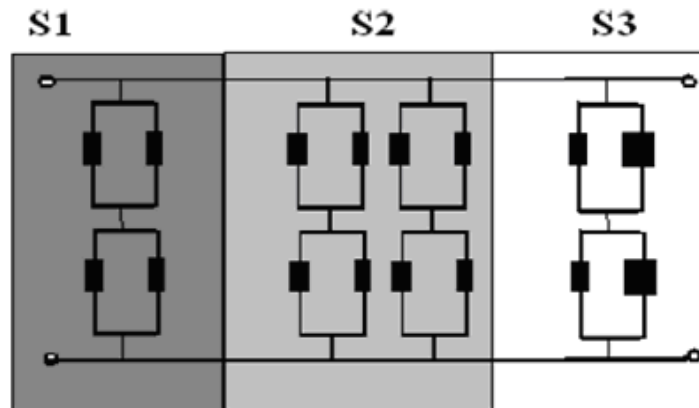
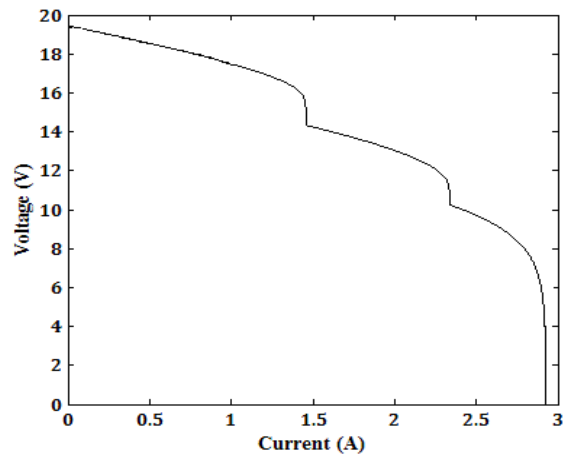


Fig.2. P-I characteristics of the solar array according to (a) the irradiation (for $T = 25^\circ C$ and different irradiation), (b) the cell temperature (for $S = 1000W / m^2$ and different temperature).

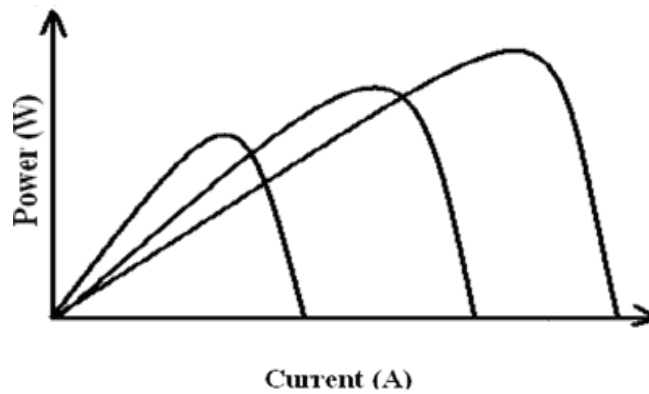
These curves show that the output power of the solar array is a nonlinear function of current and strongly influenced by irradiation and cell temperature. These figures also show that solar array maximum power and solar array current corresponding to maximum power are changed by irradiation and temperature variations. Thus utilization of a MPPT algorithm is necessary for tracking of optimum operation point of solar array. Partial shading is caused due to shadows cast by buildings, tree leaves and passing clouds. Due to partial shading, instead of a single maximum power point, a number of peaks are observed in the V-I characteristics of module.



(a)



(b)



(c)

Fig.3. (a) Different irradiation levels over a PV module, (b) V-I characteristic under partial shading condition, (c) P-I characteristics and variations of maximum power under partial shading condition.

Figs.4 and 5 show the V-I and P-I characteristics of the solar array, respectively, under uniform irradiation of $1000W/m^2$ and temperature $25^{\circ}C$. Also, these figures show the solar array characteristics under the partial shading condition. This condition is given by 5 cells with an irradiation of $800W/m^2$, temperature of $23^{\circ}C$ and 5 cells with an irradiation of $500W/m^2$ and temperature of $20^{\circ}C$.

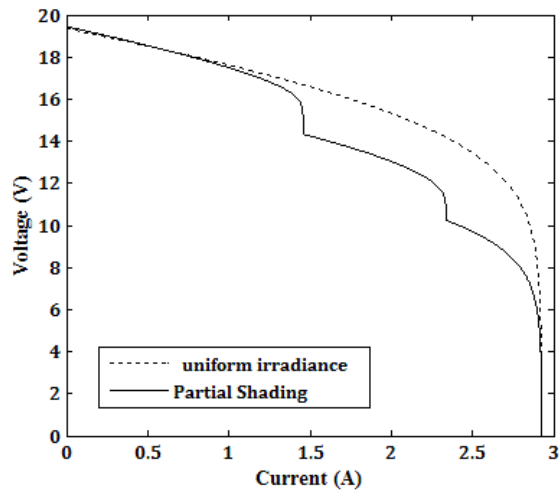


Fig. 4. V-I characteristic with and without partial shading

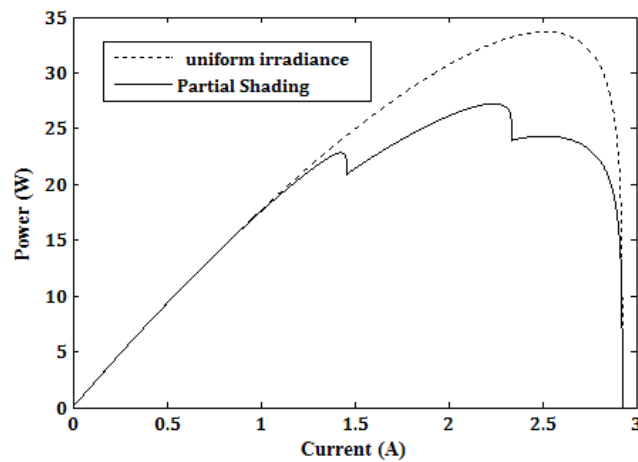


Fig.5. P-I characteristic with and without partial shading

3. Particle Swarm Optimization Concept

3.1. The Basic PSO Concept

PSO is an evolutionary computation technique for optimization of continuous nonlinear function. Kennedy and Eberhart initially proposed the PSO in 1995. Its key advantages are the ability to escape

from local maxima, easy implement and fast convergence. PSO can find the global peak and there for it is applied to determine the solar array MPP under partially shading condition.

In PSO algorithm, each particle of a swarm evaluates at different points in a D-dimensional search space and moves with a velocity according to its own previous best position (P_{best}) and its group's previous best position.

In this process, every particle in the swarm interacts with its neighbors and converges towards the global best position (where the cost function has minimum value) in the search space within a short time.

PSO consist of a swarm of particles and each particle represents a candidate solution for the optimization problem. Each particle is given with two vectors of position and velocity. The search space is D-dimensional and the position of the i_{th} particle can be represented by a D-dimensional vector $X_i = (x_{i1}, x_{i2}, \dots, x_{iD})^T$ and the velocity of this particle is $V_i = (v_{i1}, v_{i2}, \dots, v_{iD})^T$. Each particle adjusts its trajectory toward its own best previously visited position $P_i = (p_{i1}, p_{i2}, \dots, p_{iD})^T$ and the global best position of the found swarm $P_g = (p_{g1}, p_{g2}, \dots, p_{gD})^T$. The particles are updated according to the following equations:

$$v_{id} = w \times v_{id} + c_1 \times r_1 \times (p_{id} - x_{id}) + c_2 \times r_2 \times (p_{gd} - x_{id}) \quad (10)$$

$$x_{id} = x_{id} + v_{id} \quad (11)$$

Where $i = 1, 2, \dots, N$, N is the swarm size, and D is total dimension number of each particle. w Is called the inertia weight that controls the impact of previous velocity of particle on its current one. r_1 and r_2 are independently uniformly distributed random variables with range (0,1). c_1 And c_2 are the acceleration constant. A linearly decreasing inertia weight from maximum value w_{max} to minimum value w_{min} , as reflected in Eq. (12), is used to update the inertia weight as following:

$$w^k = w_{max} - ((w_{max} - w_{min}) \times k) / k_{max} \quad (12)$$

Where k_{max} is the maximum number of iterations and k is the iteration number. The PSO algorithm parameters used in this paper are presented in Table 2. These parameters are determined by trial and error method using computer simulations.

Table 2-Parameters of the PSO.

<i>Parameters</i>	<i>Value</i>
Population size	10
Dimension number	1
Maximum iteration	50
w_{\max}	0.9
w_{\min}	0.4
c_1	2
c_2	2

It is reasonable that the objective function is defined as output power of the solar array (Eq. (7)).

3.2. Improved PSO (IPSO)

Inspired by the swarm intelligence of particle swarm, a new variation of PSO is proposed in this paper. The new approach, called IPSO [23, 24], introduces two position updating strategies and a mutation operation so as to improve performance of PSO.

In general, the IPSO algorithm works as follows:

3.2.1. Initialize the problem and algorithm parameters

The problem is defined as minimize $f(x)$ subject to $x_{dL} \leq x_d \leq x_{dU}$ ($d = 1, 2, \dots, D$), x_{dL} and x_{dU} are the lower and upper bounds for decision variable x_d , and D is the dimension size of problem. The IPSO parameters are also specified in this step. They are the population size PS; decision probability L which determines different position updating strategies; mutation probability p_m ; and the maximal number of iterations (K).

3.2.2. Initialize swarm (or population)

Each initial particle in the swarm is randomly generated from a uniform distribution in the ranges $[x_{dL}, x_{dU}] (d = 1, 2, \dots, D)$. Due to the impact of the constraints; there might not be feasible solutions in the initial swarm. However, particles do not need to be initially located in feasible regions, and this is not important because of the conversion of constraints to penalty functions.

3.2.3. Position updating and mutation operation

In the IPSO model, velocity updating is excluded, and two innovative position updating strategies are introduced. The position updating of IPSO mainly works as follows: In early iterations, each particle adjusts its current position according to its previous position and its personal best position with a large probability. In other words, it is unwilling to learn from its successful companions, and it tends to adjust its current position according to its own flying experience; In late iterations, it adjusts its current position according to its previous position and the global best position with a large probability, which indicates that it prefers to imitate its successful companions in this stage. Based on the above illustration, the two position updating strategies can be formulated as follows:

$$x_{id}^{k+1} = \begin{cases} x_{id}^k + 2 \times \text{ran}_1 \times (p_{id} - x_{id}^k), & \text{if } \text{rand}(\) < L; \\ x_{id}^k + 2 \times \text{ran}_2 \times (p_{gd} - x_{id}^k), & \text{otherwise.} \end{cases} \quad (13)$$

Here, $\text{rand}(\)$, ran_1 and ran_2 are the uniformly generated random numbers in the range of $[0,1]$. Parameter L is defined as decision probability, and it is designed to be equal to $\sqrt{1 - k/K}$. According to Eq. (13), if probability L is satisfied, the current position component x_{id}^{k+1} will locate at a random position in the region $(p_{id} - |p_{id} - x_{id}^k|, p_{id} + |p_{id} - x_{id}^k|)$, which is essentially a region near personal best position component p_{id} . Otherwise, the current position component x_{id}^{k+1} will locate at a random position in the region $(p_{gd} - |p_{gd} - x_{id}^k|, p_{gd} + |p_{gd} - x_{id}^k|)$, which is essentially a region near global best position component p_{gd} . Suppose $K=1000$, then the dynamically adjusted L is depicted in Fig. 6.

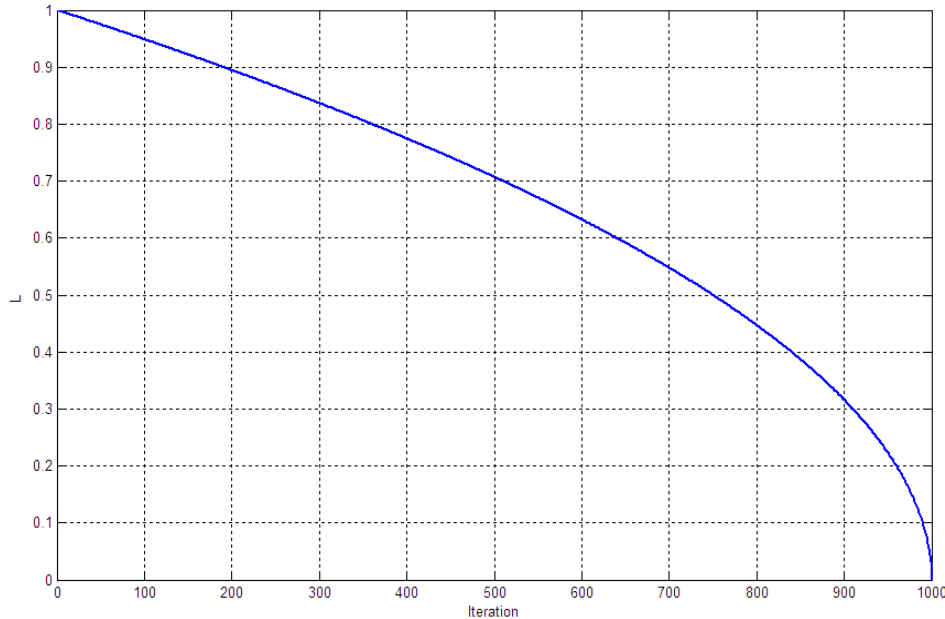


Fig. 6. Decision probability L

As can be seen from fig. 6, decision probability L decreases slowly when the number of iterations increases. A closer look at the curve reveals that L keeps to values larger than 0.5 until the current number of iterations k reaches a value larger than 700. The curve indicates that each particle using our updating strategies is more like a conservative one, and it prefers to adjust its current position according to its own experience in most iteration. It should be emphasized that the global best position is also very important for the position updating of each particle, for it provides a promising and alternative search direction for each particle. The mutation operation is carried out after updating the position, and it is used to prevent the IPSO from trapping into the local optimum.

3.2.4. Check the stopping criterion

The stopping criterion is exactly K iterations, and K is set to a fixed constant. Furthermore, if the maximal iteration number (K) is satisfied, computation is terminated. Otherwise, Step3 (3.2.6.3), is repeated. It should be noticed that there are no rules about the setting of K , and a large value is necessary to find the optimal solutions (or near optimal solutions) of reliability problems [23].

4. The proposed MPP Tracking

Fig.7 shows the configuration of the studied system. In this system, MPP tracker connects the PV module to the battery. The MPP tracker consists of boost dc-dc converter and the control system (PSO MPPT). The PSO MPPT unit uses the environmental parameters in the inputs and by using the Eqs. (1)- (9) determines current and voltage corresponding to the maximum power.

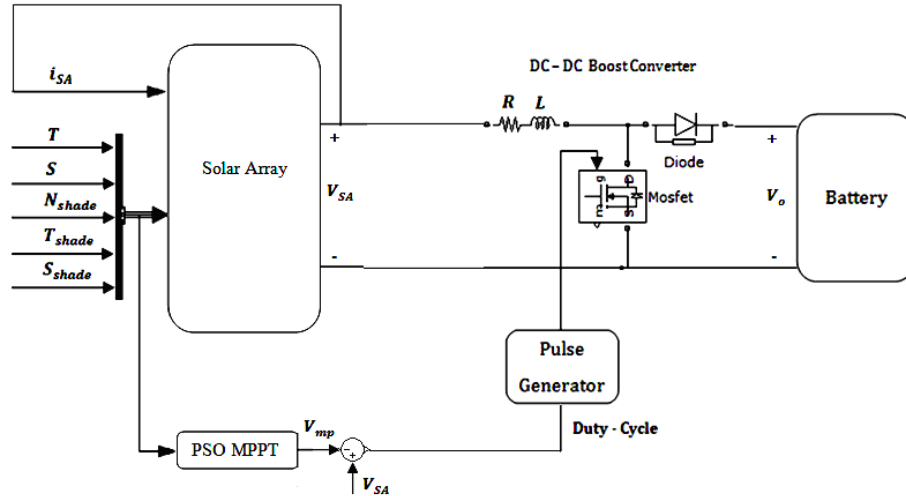


Fig. 7. System configuration.

Input of the PSO MPPT unit are the cell temperature T , the solar irradiance S , the number of shaded cells N_{shade} , the temperature of shaded cells T_{shade} and the irradiation of the shaded cells S_{shade} . The MPP tracker adjusts the operating point of the solar array to the maximum power (P_{max}) by tuning of boost converter duty cycle.

The DC/DC boost converter transfer function is obtained by considering of its steady state operation as follows:

$$V_o = \frac{V_{SA}}{1-d} \quad (14)$$

Where d is the duty cycle, V_o is the DC/DC boost converter output voltage and V_{SA} is the output solar array voltage. The optimum duty cycle (d_{opt}) is calculated from Eq.(14) with substitution of $V_{SA} = V_{mp}$ and $V_o = 25V$ (battery voltage). The flowchart of the PSO MPPT algorithm is shown in Fig. 8.

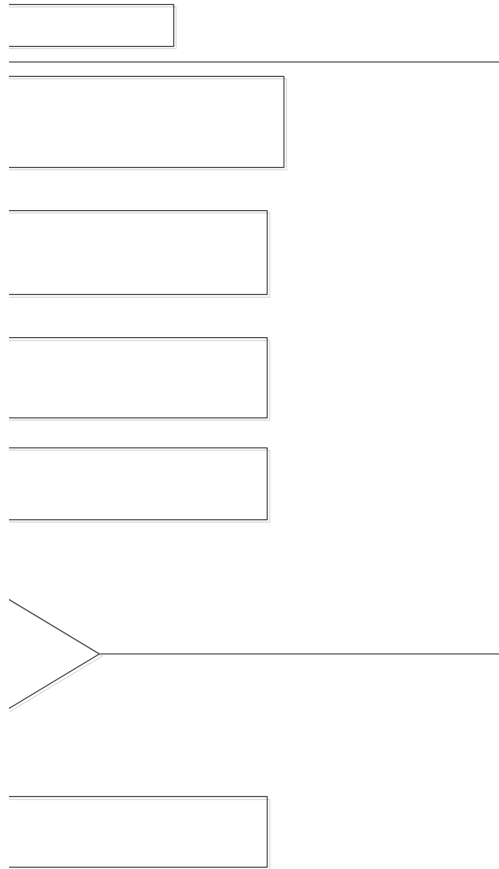


Fig. 8. Flow chart of the PSO algorithm.

To deal with dynamic shadow conditions, the PV module is logically sectioned into three sections as shown in Fig. 7. Irradiation (S) and temperature (T) data are collected at each section. This is used by the PV module in Matlab/simulink software to calculate the I_{sc} and V_{oc} of each section of the module. This data is fed to the PSO algorithm to calculate the sectional MPP voltage (V_m) and MPP current (I_m). When the value of the S and T at the i_{th} section changes, the V_{oc} and I_{sc} values also change. Thus the fitness function updates itself automatically and proceeds to find the new value of MPP of this section. It is assumed that the irradiation S and temperature conditions of a section remains unchanged while MPP of that section is being searched by the IPSO algorithm. After obtaining the MPP values of each of the independent sections, the MPP of the entire PV module is obtained from each section of the PV module.

The process repeat every time when there is a change in irradiation in any of the sections of the module. The schematic diagram of the proposed MPP tracker is shown in Fig.9.

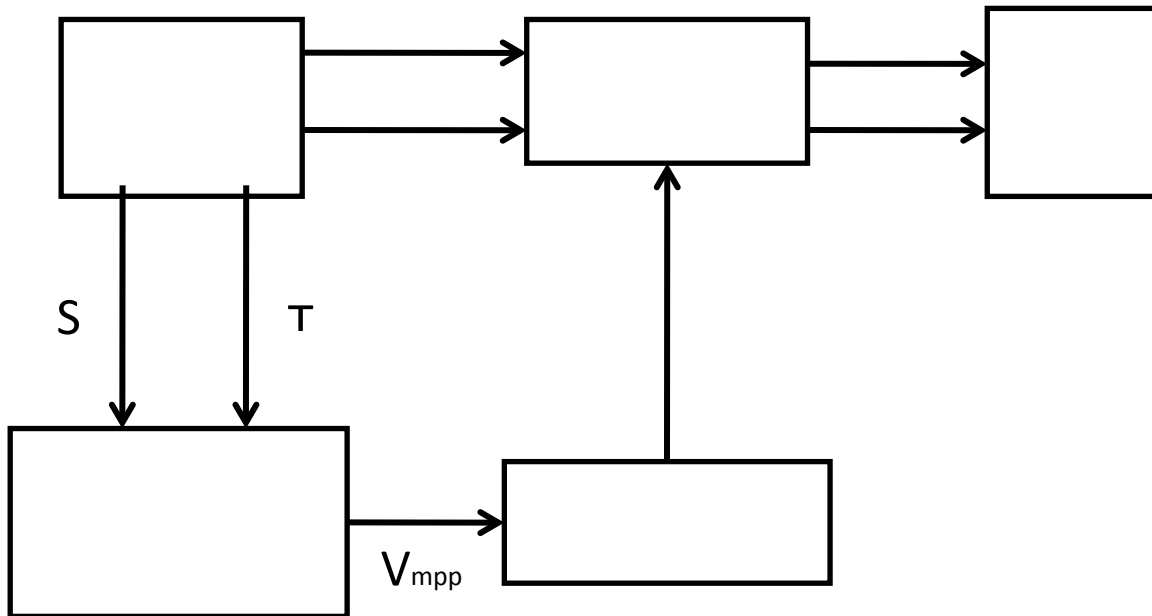


Fig. 9.Schematic diagram of proposed MPP tracker.

5. Simulation Results and Discussions

In order to investigate the accuracy and performance of the proposed method, a photovoltaic system includes: one solar panel, a DC/DC converter, a battery and control system (IPSO MPP tracker) are considered and simulated in matlab/simulink software and is shown in Fig7. The considered solar panel has one parallel string and 36 series cells per string. In order to compare performance of the IPSO MPPT algorithm, three following cases are simulated and analyzed:

Case 1- Normal operating conditions

Case 2- Partial shading conditions

Case 3- Fast variation of the cell temperature and the solar irradiance as well as partial shading conditions

5.1. Normal operating conditions

In normal operating conditions, irradiation and temperature are constant and partial shading isn't occurred. Fig.10 shows P-I characteristic of the solar array under normal operating condition. In this case, irradiation is $1000W / m^2$ and temperature is $25^{\circ}C$.

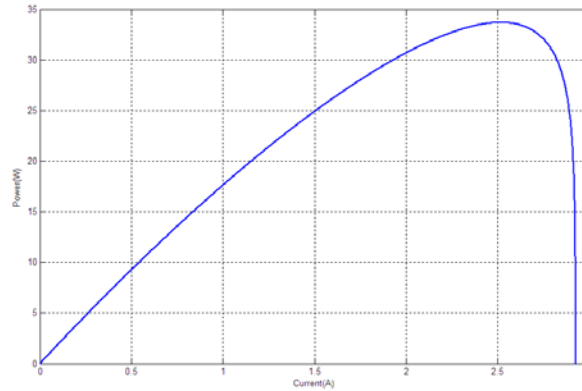


Fig. 10. P-I characteristic solar array under normal operating condition ($T = 25^{\circ}C, S = 1000W / m^2$)

Fig. 11 shows the MPPT trajectories for IPSO under normal condition.

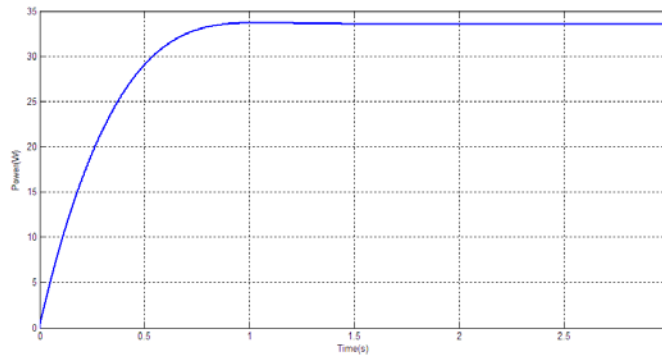


Fig. 11. The MPPT trajectories for IPSO under normal condition

5.2. Partial Shading Conditions

This investigation is implemented under partial shading condition. In this analysis, the solar irradiance and the solar array temperature of non shading solar cells are considered $1000W / m^2$ and $25^{\circ}C$, respectively. Fig. 12 shows P-I characteristic of the solar array under partial shading condition for 10 shaded cells that receive an irradiation of $500W / m^2$ and temperature $20^{\circ}C$. Fig. 13 shows the MPPT trajectories for IPSO under partial shading condition. Fig. 14 shows P-I characteristic of the solar array under partial shading condition for 20 shaded cells that receive an irradiation of $500W / m^2$ and temperature $20^{\circ}C$. Irradiation Fig. 15. Shows the MPPT trajectories for IPSO under this partial shading condition.

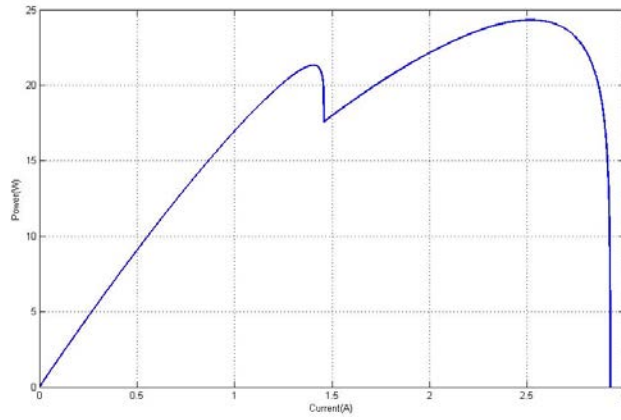


Fig. 12. P-I characteristic solar array partial shading
 $T = 25^{\circ}C, S = 1000W / m^2, N_{shade} = 10, T_{shade} = 20^{\circ}C, S_{shade} = 500W / m^2$

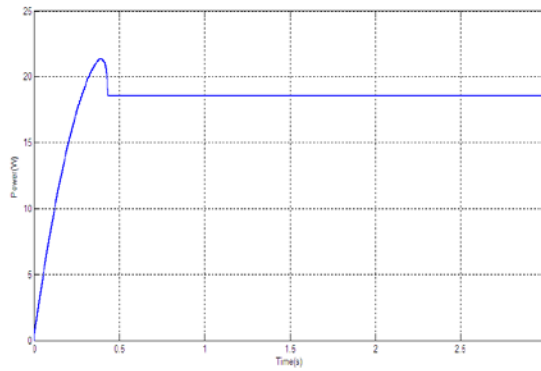


Fig. 13. The MPPT trajectories for IPSO under partial shading condition.

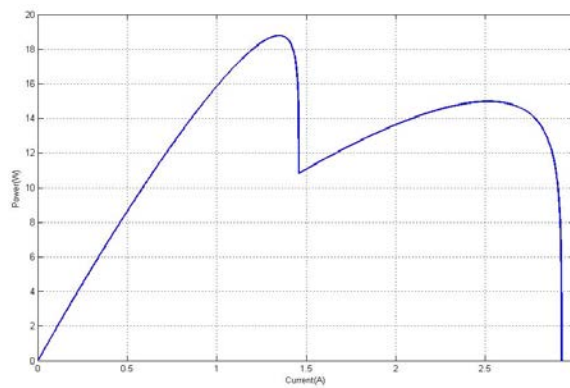


Fig. 14. P-I characteristic of the solar array under partial shading condition

$$(T=25^{\circ}C, S=1000W/m^2, N_{shade}=20, T_{shade}=20^{\circ}C, S_{shade}=500W/m^2).$$

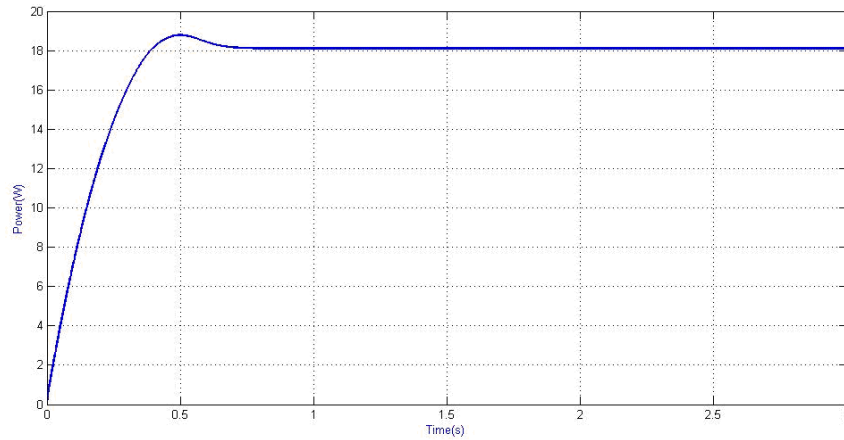


Fig. 15. The MPPT trajectories for IPSO under partial shading condition.

Fig. 16 shows P-I characteristic of solar array in irradiation of $500W/m^2$ and temperature of $25^{\circ}C$ and Fig. 17 shows P-I characteristic of solar array in irradiation of $1000W/m^2$ and temperature of $50^{\circ}C$.

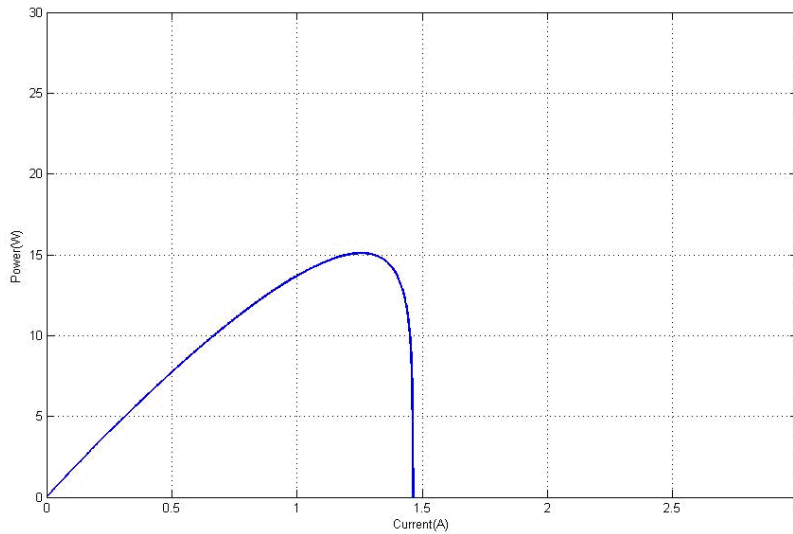
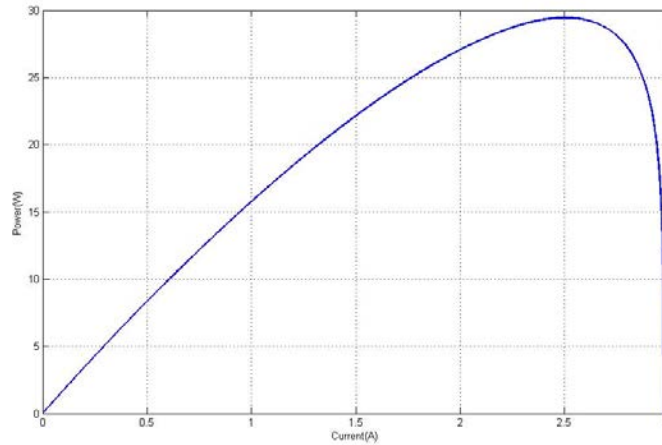


Fig. 16. P-I characteristic solar array at $S = 500W / m^2, T = 25^\circ C$.Fig. 17. P-I characteristic solar array at $S = 1000W / m^2, T = 50^\circ C$.

5.3. Fast Variations of Solar Array Temperature and Solar Irradiance as well as Partial Shading Conditions

In this case, the performance of the mentioned methods under fast variations of the solar array temperature and irradiance as well as partial shading conditions is investigated. A step change is applied to the temperature and the irradiation of shaded cells irradiation, as represented in Figs. 18-19. the output power trajectories of solar array for IPSO algorithms with $N_{shade} = 10$ are shown in Fig.20. It shows that PSO algorithm and kinds of it can find global MPP in this condition whereas studies and researches in different papers express that other

Algorithms converge to a local MPP. The above partial shading condition simulations analyses are repeated with 20 shaded cells. The output power trajectories of solar array for IPSO algorithms with $N_{shade} = 20$ are also shown in fig. 21. It shows that PSO algorithm and kinds of it can find global MPP whereas studies and researches in different papers express that other algorithms converge to a local MPP.

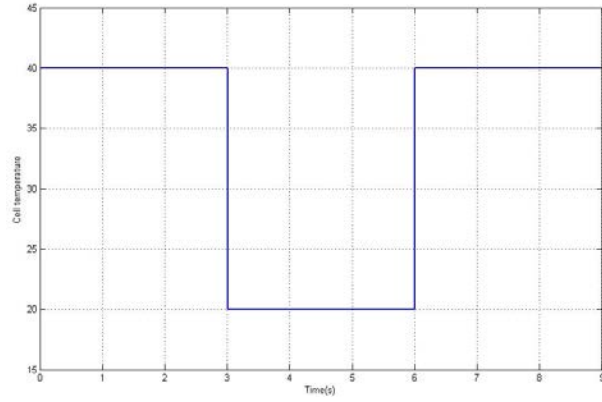


Fig. 18. Fast variations of shaded cells at temperature variations.

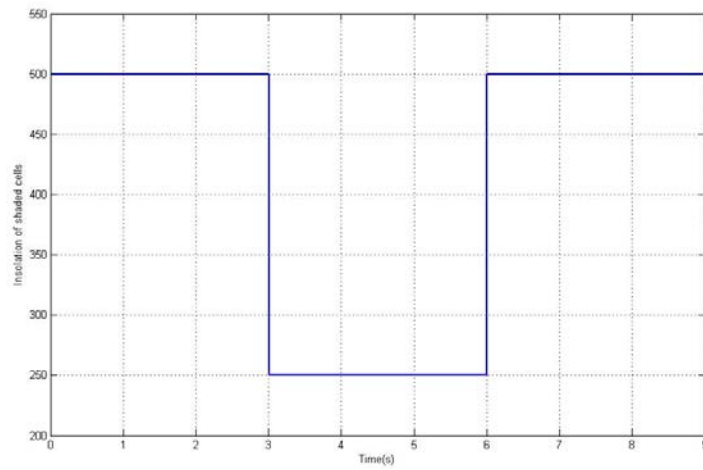


Fig. 19. Fast variations of shaded cells at irradiation variations.

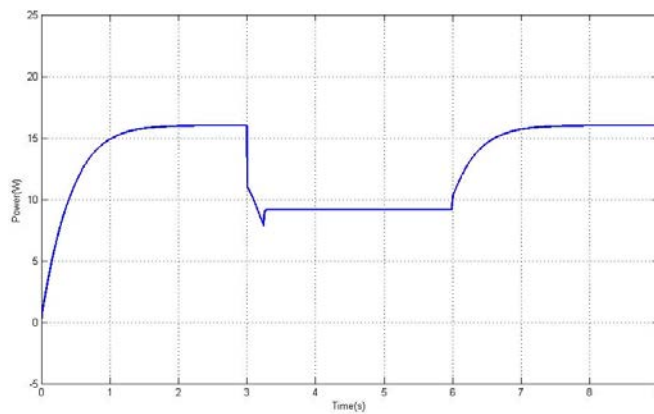


Fig. 20. The MPPT trajectories for IPSO algorithms under fast variations of solar array temperature and solar irradiance and partial shading conditions with $N_{shade} = 10$.

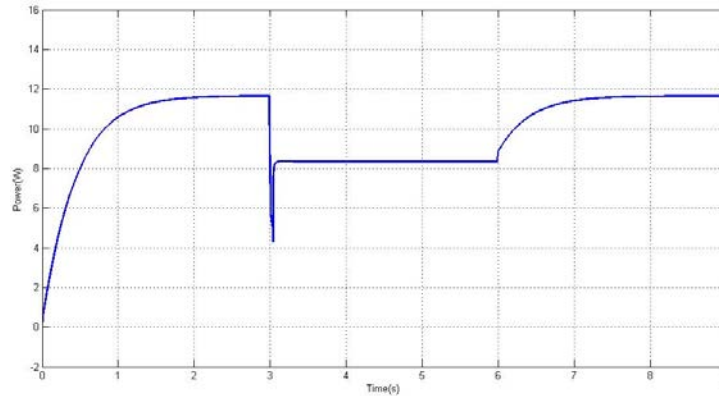


Fig. 21. The MPPT trajectories for IPSO algorithms under fast variations of solar array temperature and solar irradiance and partial shading conditions with $N_{shade} = 20$.

To evaluate the performance of the proposed PSO based MPPT algorithm and kinds of it, output power values of solar array in various operating conditions are listed in Table 3. As this table show, it is conclude that PSO algorithm with higher accuracy and better time response can track the real peak power point under different irradiation, temperature and partially shaded conditions.

Table 3

Output power values of solar array (watt) in various operating conditions

Operating conditions	Real value	IPSO	Accuracy(%)
Normal operating conditions	33.6812	33.4994	99.4
Partial shading conditions with $N_{shade} = 10$	24.3253	23.5679	96.8
Partial shading conditions with $N_{shade} = 20$	18.783	17.1081	91.08
Fast variation of the solar array temperature and solar irradiance and Partial shading conditions with $N_{shade} = 10$ at intervals of [0 3] and [6 9] second	19.9167	16.501	82.8

Fast variation of the solar array temperature and solar irradiance and Partial shading conditions with $N_{shade} = 10$ at interval of [3 6] second	10.9173	9.1686	83.9
Fast variation of the solar array temperature and solar irradiance and Partial shading conditions with $N_{shade} = 20$ at intervals of [0 3] and [6 9] second	14.3773	11.6481	81.01
Fast variation of the solar array temperature and solar irradiance and Partial shading conditions with $N_{shade} = 20$ at interval of [3 6] second	8.3544	6.8171	81.6

6. Conclusions

In this paper IPSO based MPPT and simulation results under normal and partially shaded conditions are presented. The PV curves show multiple peaks under partially shaded conditions. Results show that IPSO algorithm with high accuracy can track the real peak power point under different irradiation and temperature as well as partially shaded conditions. In addition, IPSO has a better time response and also their convergence speed is higher than other algorithms. It overcomes the weaknesses of conventional direct control method particularly in partial shading conditions. results have shown that the proposed method outperforms the conventional method in terms of tracking performance under ten different irradiance conditions, including various patterns for partial shading.

References

- [1] Kar, A., Kar, A. 2009. A New Maximum Power Point Tracking Algorithm for PV Modules under Partial Shading Rapidly Varying Illumination.
- [2] Masoum, M.A.S., Dehbonei, H., Fuchs, E.F., Theoretical and experimental analysis of photovoltaic systems with voltage and current-based maximum power point tracking. *IEEE Trans. on Energy Conversion*, 17 (2002) 514-522.
- [3] Sarvi, M., Masoum, M.A.S., Impact of Temperature and Irradiation Variation on Fuzzy MPP Tracking of Solar Panels, Proceedings of the 17th International Power System Conference, Iran, (2002) 35-45.
- [4] Qiuhua, L., Lin, Zh., Qiang, L. 2007. Simulative Research of MPPT for Photovoltaic Power System, *Electric Power Automation Equipment*, Vol.28, No.7, pp.21-25.
- [5] T.Noguchi, S.Togashi, R.Nakamoto, 2002. "Short-Current Pulse-Based Maximum-Power-Point Tracking Method for Multiple Photovoltaic and Converter Module System", *IEEE Trans. on Industrial Electronics*, Vol. 49, pp. 217-223.

- [6] Femia N, Petrone G, Spagnuolo G, Vitelli M. Optimization of perturb and observe maximum power point tracking method. *Power Electron IEEE Trans* 2005;20:963–73.
- [7] Lin C-H, Huang C-H, Du Y-C, Chen J-L. Maximum photovoltaic power tracking for the PV array using the fractional-order incremental conductance method. *Appl Energy* 2011;88:4840–7.
- [8] ESRAM T, Kimball JW, Krein PT, Chapman PL, Midya P. Dynamic maximum power point tracking of photovoltaic arrays using ripple correlation control. *Power Electron IEEE Trans* 2006;21:1282–91.
- [9] Noguchi T, Togashi S, Nakamoto R. Short-current pulse-based maximum-power-point tracking method for multiple photovoltaic-and-converter module system. *Indust Electron IEEE Trans* 2002;49:217–23.
- [10] Femia N, Granozio D, Petrone G, Vitelli M. Predictive and adaptive MPPT perturb and observe method. *Aerosp Electron Syst IEEE Trans* 2007;43:934–50.
- [12] Masoum, M.A.S., Sarvi, M. Voltage and Current Based MPPT of Solar Arrays under Variable Irradiation and Temperature Conditions, *Proceedings of International UPEC 2008, Italy, Padova*
- [13] Safari A, Mekhilef S. Simulation and hardware implementation of incremental conductance MPPT with direct control method using Cuk converter. *Indust Electron IEEE Trans* 2011;58:1154–61.
- [14] Dorofte C, Borup U, Blaabjerg F. A combined two-method MPPT control scheme for grid-connected photovoltaic systems. In: *Power electronics and applications, 2005 European conference on; 2005. p. P.1–P.10.*
- [15] Rai AK, Kaushika ND, Singh B, Agarwal N. Simulation model of ANN based maximum power point tracking controller for solar PV system. *Sol Energy Mater Sol Cell* 2011;95:773–8.
- [16] Kobayashi K, Takano I, Sawada Y. A study of a two stage maximum power point tracking control of a photovoltaic system under partially shaded insolation conditions. *Sol Energy Mater Sol Cell* 2006;90:2975–88.
- [17] Karatepe E, Hiyama T, Boztepe M, Çolak M. Voltage based power compensation system for photovoltaic generation system under partially shaded insolation conditions. *Energy Convers Manage* 2008;49:2307–16.
- [18] Miyatake M, Inada T, Hiratsuka I, Hongyan Z, Otsuka H, Nakano M. Control characteristics of a fibonacci-search-based maximum power point tracker when a photovoltaic array is partially shaded. In: *4th International on power electronics and motion control conference, vol. 2; 2004. p. 816–21.*
- [19] Patel H, Agarwal V. Maximum power point tracking scheme for PV systems operating under partially shaded conditions. *Indust Electron IEEE Trans* 2008;55:1689–98.
- [20] Tat Luat N, Kay-Soon L. A global maximum power point tracking scheme employing DIRECT search algorithm for photovoltaic systems. *Indust Electron IEEE Trans* 2010;57:3456–67.

- [21] Salem F, Adel Moteleb Mohamed S, Dorrah HT. An enhanced fuzzy-PI controller applied to the MPPT problem. *J SciEng* 2005;8:147–53.
- [22] Eberhart R, Kennedy J. A new optimizer using particle swarm theory. In: *Micromachine and human science, 1995. MHS '95' Proceedings of the sixth international symposium on*; 1995. p. 39–43.
- [23] Wu, P., Gao, L., Zou, D., Li, S. 2011. An Improved Particle Swarm Optimization algorithm for reliability problems.
- [24] Fang, H., Chan, L., Shen, Z. 2011. Application of an improved PSO algorithm to optimal tuning of PID gains for water turbine governor. Omkar, S.N., Mudigere, D., NarayanaNaik, G., Gopalakrishnan, S. 2007. *Vector* .
- [25] Matsuo, H., Lin, W., Kurokawa, F. 2004. Characteristics of the Multiple-Input DC-DC Converter. *IEEE Trans on IE*, Vol.51, No.3, pp.625–631.
- [26] Esmar T, Chapman PL. Comparison of photovoltaic array maximum power point tracking techniques. *Energy Convers IEEE Trans* 2007;22:439–49.
- [27] Young-Hyok J, Doo-Yong J, Jun-Gu K, Jae-Hyung K, Tae-Won L, Chung-Yuen W. A real maximum power point tracking method for mismatching compensation in PV array under partially shaded conditions. *Power Electron IEEE Trans* 2011;26:1001–9.
- [28] Ishaque K, Salam Z, Taheri H, Syafaruddin. Modeling and simulation of photovoltaic (PV) system during partial shading based on a two-diode model. *Simul Mod PractTheor* 2011;19:1613–26.
- [29] Patel H, Agarwal V. MATLAB-based modeling to study the effects of partial shading on PV array characteristics. *Energy Convers IEEE Trans* 2008;23:302–10.
- [30] User's Manual. Programmable photovoltaic array simulator PVAS1. Arsenal Research, Austrian Institute of Technology (AIT); 2007.
- [31] Ishaque K, Salam Z, Taheri H. Accurate MATLAB simulink PV system simulator based on a two diode model. *J Power Electron* 2011;11:9.
- [32] Zain-Ahmed A, Sopian K, ZainolAbidin Z, Othman MYH. The availability of daylight from tropical skies – a case study of Malaysia. *Renew Energy* 2002;25:21–30.
- [33] Azli NA, Salam Z, Jusoh A, Facta M, Lim BC, Hossain S. MPPT performance of a grid-connected PV inverter under Malaysian conditions. In: *Power and energy conference, 2008. PECon 2008. IEEE 2nd international*; 2008. p. 457–9.
- [34] HamzeRavaee, SaeidFarahat, FaramarzSarhadd. Artificial Neural Network Based Model of Photovoltaic Thermal (PVT) Collector. "Journal of mathematics and computer Science" Volume: 4 (2012) Issue: 3, Pages: 411 – 417.
- [35] MahbubehMoghaddas, MohamadRezaDastranj, NematChangizi, ModjtabaRouhani. PID Control of DC motor using ParticleSwarmOptimization PSO Algorithm. "Journal of mathematics and computer

Science"Volume: 1 (2010) Issue: 4 Pages: 386 - 391

[36]Hamid Reza Feili, FatemehMoghadasi, ParisaNaderipour. Optimization of Solar Cooling Systems with Simulation Modeling . "Journal of mathematics and computer Science"Volume: 6 (2013) **Issue:** 4 Pages: 286 - 291